

Aerosol dynamical model MULTIMONO

Liisa Pirjola and Markku Kulmala

Department of Physics P.O. Box 9, FIN-00014 University of Helsinki, Finland

Pirjola, L. & Kulmala, M. 2000. Aerosol dynamical model MULTIMONO. *Boreal Env. Res.* 5: 361–374. ISSN 1239-6095

We have developed two effective aerosol dynamical models MULTIMONO and MONO32. The models take into account gas-phase chemistry and aerosol dynamics and includes the following processes: (1) emissions of gases and particles; (2) chemical reactions in the gas phase; (3) dry deposition of gases and particles; (4) homogeneous binary $\text{H}_2\text{SO}_4\text{-H}_2\text{O}$ or ternary $\text{H}_2\text{SO}_4\text{-H}_2\text{O-NH}_3$ nucleation; (5) multicomponent condensation of H_2SO_4 , H_2O , HNO_3 , NH_3 and some organic vapour X onto particles; and (6) inter- and intramode coagulation of particles. The particles can be classified into four different size modes which are monodisperse (all particles in a mode possess the same size and composition). In these models the different aerosol properties, such as the particle number concentration, the particle diameter, the mass and composition of the whole distribution, and the mass of particulate matter smaller than $2.5\ \mu\text{m}$ ($\text{PM}_{2.5}$) and smaller than $10\ \mu\text{m}$ (PM_{10}) can be studied. Particles can include soluble material such as sulphate, nitrate, ammonium, and sodium chloride, as well as insoluble material such as organic carbon, elemental carbon, and mineral dust. We have chosen five different particle classes for each size mode (MULTIMONO), or assumed internally-mixed particles (MONO32). The developed models have been compared with a more detailed sectional model AEROFOR2. The comparison shows that the developed models are physically sound. The performed model runs show that the composition of aerosol particles depends mainly on emissions and condensation. Coagulation seems to be of minor importance. The state of mixing can be studied effectively using MULTIMONO or MONO32. E.g. the degree of internal mixing depends on the condensation rate and condensation time. The developed models can be used as sub-models in one-dimensional boundary layer models and three-dimensional Eulerian models.

Introduction

Atmospheric aerosol particles influence Earth's radiation balance directly by scattering and absorbing solar radiation, and indirectly by acting as cloud condensation nuclei (CCN) (e.g. Charlson

et al. 1992). Recently some progress has been made in evaluating the radiative effects of various aerosol components such as sulfate, organics, black carbon, sea salt, and crustal species (Sokolik and Toon 1996, Chuang *et al.* 1997, Kaufman and Fraser 1997, Winter and Chylek

1997, Haywood and Ramaswamy 1998). However, substantial uncertainties still remain in the significance of both direct and indirect radiative forcing due, for example to biogenic emissions of organic vapours.

On the other hand, atmospheric aerosol particles in urban areas cause the loss of visibility (e.g. Finlayson-Pitts and Pitts 2000) and influence the human health (Dockery and Pope 1994). Heavily industrialized areas suffer from pollution fogs (smogs) that are often related to coal burning and nowadays also to traffic. The most well-known example of such smogs is the London "pea-souper" smog which occurred every once in a while until the 50's, when the coal burning was forbidden. Besides visibility degradation, the London smog episodes caused serious health effects and "excess deaths". One significant part of the health problems were atmospheric aerosols and fog droplets, since particles having diameters less than 10 μm can penetrate deep into the respiratory system (Dockery and Pope 1994).

The increased aerosol concentrations are largely due to secondary particle production, i.e. homogeneous nucleation from vapours. Instrumental techniques for measuring the concentration of freshly-formed particles have been developed recently, so that particles with a diameter of about 3 nm can be detected. Particles of this small size have been observed in the free troposphere (Clarke 1992, Schröder and Ström 1997, Raes *et al.* 1997), in the marine boundary layer (Covert *et al.* 1992, Hoppel *et al.* 1994, O'Dowd *et al.* 1998), in the vicinity of evaporating clouds (Hegg *et al.* 1991), in Arctic areas (Wiedensohler *et al.* 1996, Pirjola *et al.* 1998), in urban areas and in stack plumes (Kerminen and Wexler 1996), and recently also in boreal forests (Mäkelä *et al.* 1997).

Although the ternary nucleation of sulphuric acid, ammonia, and water can explain the aerosol formation in many cases (Kulmala *et al.* 2000), some other condensable vapour is needed for explaining the aerosol growth and the aerosol mass and composition distributions. Recently Kerminen *et al.* (1999) and Kulmala *et al.* (1998a) have discussed the importance of organic vapours to the aerosol growth. Also the importance of sulphate surface chemistry to the aerosol mass distribution has been investigated (Kerminen *et al.* 2000a).

The complexity of aerosol processes in the

development of aerosol number and mass concentrations and the aerosol composition is huge. Therefore, simple and computationally effective, yet physically sound models are needed. Recently, Ackermann *et al.* (1998) presented a modal approach which can be used to simulate the particle formation, transportation, and deposition in regional chemical transport models. In their approach, the particles could consist of sulphate, nitrate, ammonium, and water. Harrington and Kreidenweiss (1998a, 1998b) applied a mono-disperse modal approach to model sulphate particles.

In the present paper we develop a simple and effective model, MULTIMONO, that simulates the formation and subsequent growth of aerosol particles, and evaluates the number and mass concentrations of different types of particles. All the main aerosol physical processes (nucleation, condensation, coagulation, deposition, and emissions), together with the gas-phase chemistry, are included. One of the main aims in our model development is to find out an effective but a physically sound model to be used as a subroutine in three-dimensional Eulerian models.

The MULTIMONO model and a simplified version of it, MONO32 (section 4), can be used to investigate the role of different emissions in determining the concentration and composition of the particles. Examples are the role of biogenic emissions in atmospheric CCN production, and interactions between biogenic aerosols and anthropogenic pollutants. This paper emphasizes the influence of coagulation and condensation, even though also dry deposition and chemistry are taken into account. We further investigate how rapidly the aerosol composition changes as a function of condensable vapour concentrations and a pre-existing aerosol particle concentration. The comparison of the developed model with a more detailed sectional model AEROFOR2 (Pirjola and Kulmala 2000) is also presented.

Model description

In the present work we have developed an effective aerosol dynamical model MULTIMONO, which is based on our earlier version of a mono-disperse aerosol dynamical model (Kulmala *et al.*

1995, Pirjola and Kulmala 1998). The model takes into account gas-phase chemistry and aerosol dynamics, including the following processes: (1) emissions of gases and particles; (2) chemical reactions in the gas phase; (3) dry deposition of gases and particles; (4) homogeneous binary $\text{H}_2\text{SO}_4\text{-H}_2\text{O}$ or ternary $\text{H}_2\text{SO}_4\text{-H}_2\text{O-NH}_3$ nucleation; (5) multicomponent condensation of H_2SO_4 , H_2O , HNO_3 , NH_3 and some organic vapour X onto particles, and (6) inter- and intramode coagulation of particles.

The particles belong to one of the four size modes called the nucleation, the Aitken, the accumulation, and the coarse mode. The initial diameter of particles belonging to these modes may vary in the ranges 1–20 nm, 20–100 nm, 100 nm–2.5 μm , and > 2.5 μm , respectively. This definition allows us to study the properties, such as the particle number concentration, the particle diameter, and the mass and composition of particulate matter smaller than 2.5 μm ($\text{PM}_{2.5}$) and smaller than 10 μm (PM_{10}). Besides, emissions of particles are measured in $\text{PM}_{2.5}$ and PM_{10} . The particles grow by coagulation and condensation inside the mode and thus the radius of each mode increases. How and when the particles in a mode have grown so large that it is reasonable to move them to the following mode is a future work.

The particles can contain soluble material such as sulphate, nitrate, ammonium, sodium chloride (and organics), as well as insoluble material such as elemental or organic carbon, and mineral dust. We have chosen five particle composition classes within the each size mode (Table 1). At the beginning of the simulation the particles can be pure sulphuric acid-water particles, pure organic or elemental carbon particles, pure sea salt particles, pure dust particles, or mixtures of some of these. After the growth processes the particle composition changes. Since pure nitrate or pure ammonium particles cannot exist, sulphate, nitrate, and

ammonium are lumped together as inorganic salts.

The differential equations for the number concentration N_i and total mass concentrations in each mode M_i are:

$$\frac{dN_i}{dt} = \text{nucleation} + \text{emission} - \text{coagulation} - \text{drydeposition} \quad (1)$$

$$\frac{dM_i}{dt} = \text{nucleation} + \text{emission} \pm \text{coagulation} \pm \text{condensation} - \text{drydeposition} \quad (2)$$

The total mass includes the mass of sulphate, nitrate, ammonium, organic and elemental carbon, sea salt, mineral dust, and water. To follow the composition (the mass fraction) of particles, we need separate differential equations for the mass of each chemical component, so that the total mass becomes the sum of the masses of these components. Thus the total number of differential equations is 68 (chemistry) + 20 (the particle number concentration) + 7×20 (the mass concentrations of sulphate, nitrate, ammonium, organic and elemental carbon, sea salt, and mineral dust) = 68 + 160. The set of equations is solved numerically with a NAG-library FORTRAN-routine DO2EJF (1990).

Gas-phase chemistry

The chemistry mechanism is based on an EMEP mechanism (Simpson 1992). It includes 68 chemical compounds (inorganic and organic) and 140 chemical or photochemical reactions (Pirjola and Kulmala 1998), and is capable of simulating rural, urban, and marine conditions. The initial concentration, the emission rate, and the deposition velocity of each compound are given as an input to the model.

Table 1. Size modes and particle types in the model.

	Sulphate/ Nitrate/ Ammonium	Organic carbon	Elemental carbon	NaCl	Mineral dust
Nucl. Mode	X	X			
Aitken mode	X	X	X	X	
Accum. mode	X	X	X	X	X
Coarse mode	X	X	X	X	X

Nucleation

The binary $\text{H}_2\text{SO}_4\text{-H}_2\text{O}$ nucleation rate is determined by applying the revised classical nucleation theory (Wilemski 1984) which is thermodynamically correct, and by taking into account the hydrate formation (Jaecker-Voirol *et al.* 1987). This form of theory predicts quite well the homogeneous nucleation in a sulphuric acid-water system at a temperature of around 289 K and at relative humidities of 30%–50% (Viisanen *et al.* 1997). To save the computer time, we have used a parameterised value for the sulphuric acid mole fraction in the critical nucleus as a function of temperature, relative humidity, and relative acidity, as described in Kulmala *et al.* (1998b).

Several field measurements indicate that the observed ambient nucleation rates substantially exceed those predicted by the binary $\text{H}_2\text{SO}_4\text{-H}_2\text{O}$ nucleation theory (Covert *et al.* 1992, Weber *et al.* 1998, 1999, O'Dowd *et al.* 1998, 1999, Clarke *et al.* 1999). The recently developed classical theory for ternary $\text{H}_2\text{SO}_4\text{-NH}_3\text{-H}_2\text{O}$ nucleation (Korhonen *et al.* 1999) shows that if the NH_3 concentration is over 100 parts per trillion (ppt) and the H_2SO_4 concentration is equal to 10^6 molecules cm^{-3} , a significant nucleation can occur. On the other hand if the H_2SO_4 concentration exceeds 10^7 molecules cm^{-3} , around 20 ppt of NH_3 is needed for a significant nucleation to occur. A preliminary parameterisation for the ternary nucleation rate is available in MULTIMONO.

Condensation

The molecular and the mass flux of condensing sulphuric acid and organic vapours depends on the difference between the vapour concentration far from the droplet and that at the droplet surface, on the diffusion coefficient, and on the condensational sink due to pre-existing particles. We used the continuum regime theory corrected by a transitional correction factor (Fuchs and Sutugin 1970, *see also* Pirjola *et al.* 1999). The molecular diffusion coefficient can be estimated using empirical correlations given by Reid *et al.* (1987). It should be noted that under tropospheric conditions, the saturation vapour pressure of sulphuric acid is much lower than its ambient va-

pour pressure, so that its evaporation from a particle is negligible. Depending on its saturation vapour pressure, an organic vapour can be non-volatile, semivolatile, or highly volatile. The majority of organics identified up to now in atmospheric particles are semivolatile or highly volatile (e.g. Hoffmann *et al.* 1998, Griffin *et al.* 1999, Jang and Kamens 1999). However, typically only about 10% of the organic aerosol mass has been identified (Saxena and Hildemann, 1996). Therefore, it is possible that some of these unidentified multifunctional compounds are nonvolatile and thus able to grow nanometer-size particles to a CCN size, as demonstrated by Kerminen *et al.* (2000b). In this work organic vapours are assumed to be nonvolatile.

At the moment, the condensation of nitric acid is treated in a similar way as the condensation of sulphuric acid.

The condensation of ammonia is coupled to the concentration of H_2SO_4 and HNO_3 (Seinfeld and Pandis 1998). If possible, each condensing H_2SO_4 molecule removes two NH_3 molecules from the gas phase, which leads to the formation of ammonium sulphate ($\text{NH}_4)_2\text{SO}_4$. If there is excess NH_3 available, it can react with nitrate to produce NH_4NO_3 , and each HNO_3 molecule takes one NH_3 molecule when condensing.

The water content of aerosols (*see* <http://www.epa.gov/asmdnerl/models3/>) is calculated using empirical polynomials (Tang and Munkelwitz 1994) for the mass fraction of solute as a function of water activity. The polynomials for ammonium nitrate and ammonium sulphate are taken from Chan *et al.* (1992). The chemical composition of a sulphate-nitrate-ammonium-water aerosol is based on equilibrium thermodynamics. The amount of water depends on the molar concentration ratio between the total ammonia and the total sulphate: if this ratio is < 2 the aerosol phase includes ammonium sulphate, and if it is ≥ 2 all the sulphate is ammonium sulphate and the excess ammonium forms ammonium nitrate. The organic vapour in the aerosol phase is assumed not to uptake water, so the hygroscopic properties of particles are determined by inorganic salts. This is probably a reasonable approximation for most organics in atmospheric aerosols (e.g. Saxena and Hildemann 1997, Virkkula *et al.* 1998, Dick *et al.* 2000).

Sea salt particles are hygroscopic and their

contribution to the total water content is significant. A value of 2.0 to the growth factor corresponding to 90% relative humidity is used in calculating the wet radius of sea-salt particles and the mass of associated water.

Coagulation

Brownian coagulation coefficients K_{ij} between particles in modes i and j are calculated according to Fuchs (1964). If there are particles larger than a few micrometers in diameter, gravitational coagulation becomes important (e.g. Seinfeld and Pandis 1998) and is also taken into account. When two particles belonging to different particle composition classes coagulate, the resulting particle is put to the composition class of the originally larger particle. If the coagulating particles are of the same size, then half of the resulting particles are partitioned to each composition classes.

Dry deposition

Dry deposition rates of particles are modelled according to Schack *et al.* (1985). Brownian diffusion, interception, and gravitational settling are taken into account.

Simulating coagulation and condensation with MULTIMONO

Under typical atmospheric conditions, we simulated aerosol particle populations containing sulphate particles from anthropogenic pollutants or from natural DMS sources, and organic particles

of biogenic origin. The changes in the particle number concentration and composition as a function of the condensable vapour concentration and the initial particle number concentration was investigated. At the beginning of each 24-hour simulation, the aerosol population was assumed to be an external mixture of pure sulphuric acid-water particles and organic particles in both the Aitken and the accumulation mode. The initial particle dry diameter was 20 nm for the Aitken mode and 100 nm for the accumulation mode. The temperature and relative humidity were kept constant and equal to 293 K and 50%, respectively.

The effect of coagulation was studied by setting the condensing vapour concentrations to zero and by varying the total aerosol number concentration N_{tot} . The concentration ratio between sulphate and organic particles was 10:1, even though the simulations were repeated using the ratios 1:1 and 1:10. Of both sulfate and organic particles, 80% were assumed to be in the Aitken mode and 20% in the accumulation mode. Table 2 summarizes the initial and final aerosol concentrations in the sulphate and organic modes.

If the initial N_{tot} was 10^3 cm^{-3} , coagulation was very slow and the particle number concentrations reduced slightly (Fig. 1) Especially the accumulation mode particle concentrations remained practically constant. If the initial N_{tot} was 10^4 or 10^5 cm^{-3} , coagulation removed about 60% and 90% of the particles, respectively. The organic Aitken mode particle concentration decreased faster than the corresponding sulphate particle concentration. This is due to the smaller size of organic particles, since they are assumed to be insoluble and to absorb no water. When a smaller organic Aitken mode particle coagulates with a sulfate Aitken mode particle, the resulting particle is classified

Table 2. Initial and final particle concentrations (cm^{-3}) for ratios of sulphate and organic particles equal to 10:1, 1:1 and 1:10. N_{sa} refers to originally pure sulphuric acid-water particles and N_{org} to pure organic particles.

	N_{tot}	N_{sa}	N_{org}	N_{tot}	N_{sa}	N_{org}	N_{tot}	N_{sa}	N_{org}
Initial	10^3	910	90	10^3	500	500	10^3	90	910
Final	856	787	69	848	447	401	845	83	762
Initial	10^4	9 100	900	10^4	5 000	5 000	10^4	900	9 100
Final	3 954	3 554	199	3 579	2 261	1 318	3 484	490	2 994
Initial	10^5	91 000	9 000	10^5	50 000	50 000	10^5	9 000	91 000
Final	9 987	9 621	365	9 593	6 747	2 846	9 376	1 683	7 693

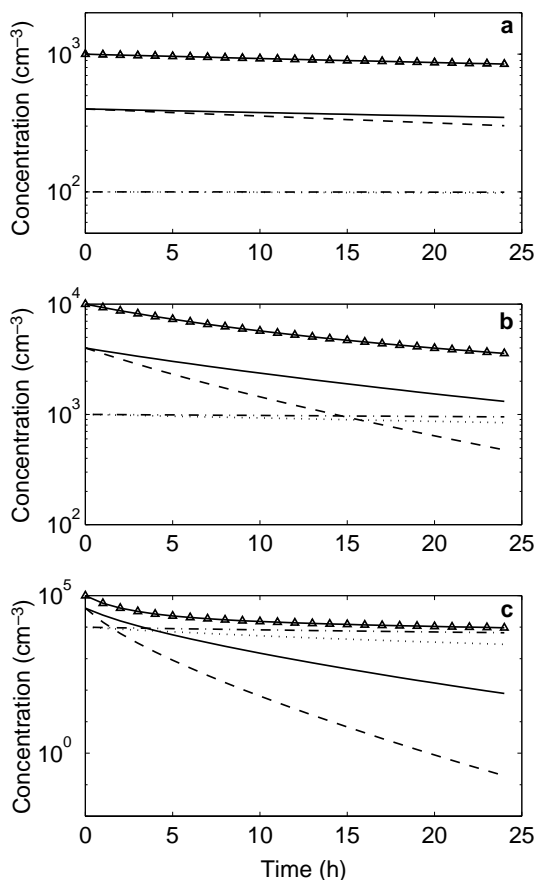


Fig. 1. Time evolution of the total number concentration N_{tot} (curve with triangles), the number concentration of sulphate Aitken and accumulation mode particles (solid and dash-dot curves), as well as the number concentration of organic Aitken and accumulation mode particles (dashed and dotted curves). The initial N_{tot} is 10^3 cm^{-3} (a), 10^4 cm^{-3} (b) and 10^5 cm^{-3} (c), and is distributed equally between the sulphate and the organic particles.

as a sulfate Aitken mode particle. This kind of behaviour is not so clear for the accumulation mode because coagulation is slower there due to the larger particle size.

Figure 2 gives an example on how the composition of particles changes during the coagulation process. The composition of organic particles changed very little in the accumulation mode and not at all in the Aitken mode. Because Aitken mode organics particles are the smallest particles, their coagulation with a sulphate particle always results in an Aitken or a accumulation mode sulphate particle. The sulphate mass fraction of ac-

cumulation mode organic particles increases when they coagulate with sulphate Aitken mode particles, whereas the organic mass fraction of accumulation mode sulphate particles increases when they coagulate with organic Aitken or accumulation mode particles. Naturally, self-coagulation does not change the composition of particles in any mode.

The greater the initial N_{tot} , the faster the sulphate mass fraction of particles decreased and the respective organic mass fraction increased. This behaviour naturally depends on the initial ratio of the number of sulphate and organic particles. If the sulphate particles were the dominant ones, then the sulphate mass fraction of sulphate particles decreased slower and the organic mass fraction of organic fraction decreased faster than what is seen in Fig. 2. If the organic particles were dominant ones, the composition of pure sulphate particles changed to organic direction faster than in Fig. 2, and the composition of pure organic particles remained more than 99.5% of organic.

When condensable vapours were present, the changes in the particle composition were found to depend on the amount of the vapours, the fraction of sulphuric acid and organics, and the initial particle size distribution (Figs. 3–5). Simulations in Figs. 3–5 were performed assuming an initial N_{tot} of 1000 cm^{-3} , so the effect of coagulation played an insignificant role. The initial number concentration of sulphate particles was ten-fold to compared with the concentration of organic particles, but this concentration ratio was found to have no effect on the final particle composition. This was also true for the initial N_{tot} equal to 10^4 cm^{-3} or 10^5 cm^{-3} , in which cases coagulation gives an additional contribution to the particle number and composition development. The steady state composition was reached more rapidly when more condensable vapours were available. For example, for the condensable vapour concentration of $10^9 \text{ molecules cm}^{-3}$ the steady state is reached in an hour, for the concentrations of $10^8 \text{ molecules cm}^{-3}$ it takes about 3 hours, and for the concentration of $10^7 \text{ molecules cm}^{-3}$ more than 24 hours. The simulations were repeated for higher particle number concentrations and it was found that the final sulphate and organic mass fractions were independent of the initial particle concentration, at least with the used vapour concentrations of

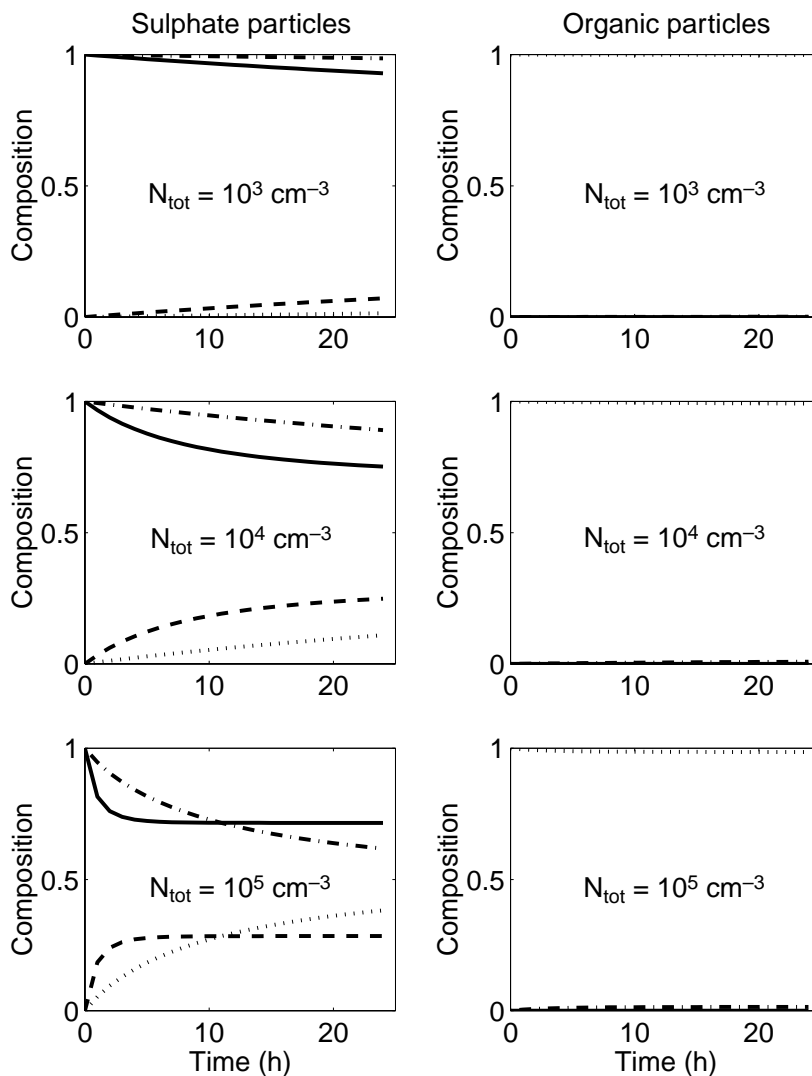


Fig. 2. Time evolution of the composition of originally pure sulphate particles and pure organic particles assuming the total particle number concentrations of 10^3 , 10^4 , or 10^5 cm^{-3} . Solid curves refer to the Aitken mode and dash-dot curves to the accumulation mode sulphate mass fractions. Dashed curves refer to the Aitken mode and dotted curves to the accumulation mode organic mass fractions. The original ratio of pure sulphate and organic particles is 1:1.

10^7 – 10^9 molecules cm^{-3} . Thus, we can conclude that in these cases, condensation modified the particle composition stronger than what coagulation did.

It can clearly be seen that when the concentration of condensable vapours was high (Fig. 5), an originally externally-mixed particle population became internally mixed, i.e. the composition of sulphate and organic particles became identical after a couple of hours. On the other hand, if the concentration of condensable vapours was low enough (e.g. Fig. 3), originally internally-mixed particles such as sulphate particles were transformed externally mixed.

The relative humidity RH had a weak influ-

ence on the results shown in Figs. 1–5. The higher the RH, the larger the water content of particles and the smaller the coagulation rate. Consequently, the total number concentration at the end of the simulation was 3.5% larger for the RH = 90% than for the RH = 50%, and 3.5% smaller for the RH = 10% than for the RH = 50%. Since the sulphate and organic mass fractions are calculated without water, and since coagulation has only a minor effect on composition, changes in the relative humidity have practically no influence on the particle composition.

The time development of the particle size is shown in Fig. 6. It should be noted that if the vapour concentration was 10^8 molecules cm^{-3} , both

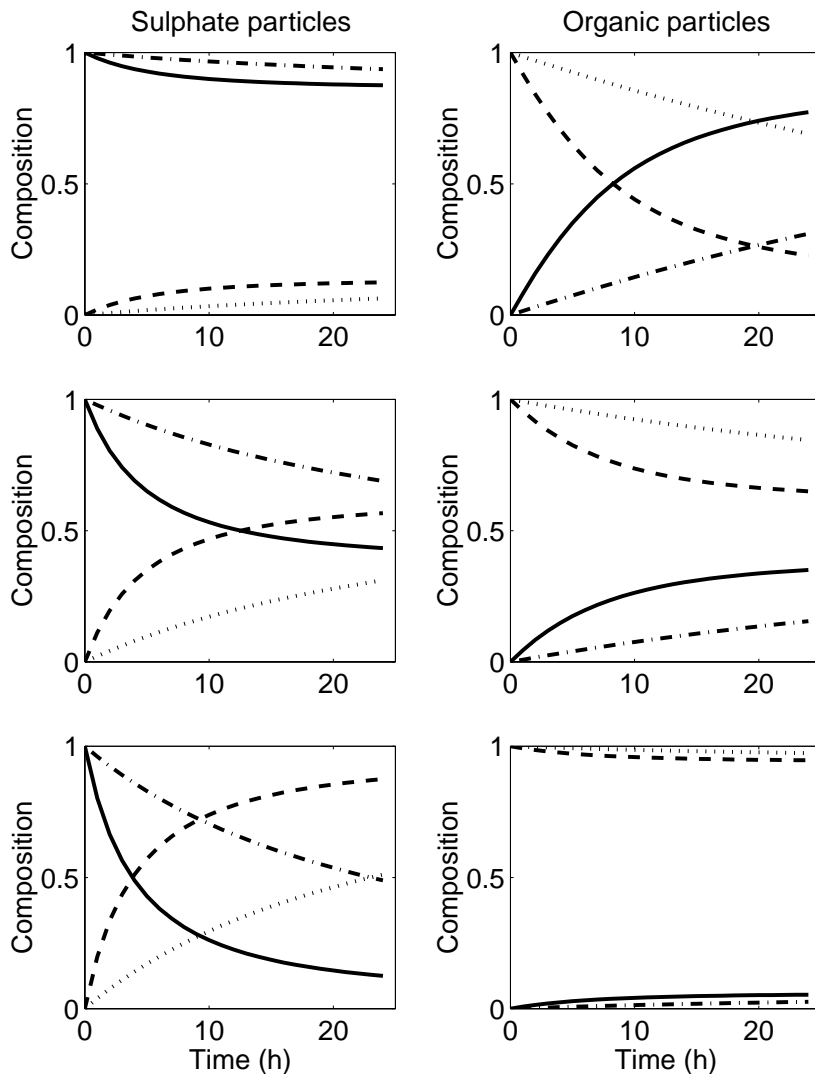


Fig. 3. Time evolution of the composition of originally pure sulphate and pure organic particles when the total condensable vapour concentration is equal to 10^7 molecules cm^{-3} . The concentration ratio between the sulphuric acid and the organic vapours is 10:1 (the uppermost figures), 1:1 (the middle ones), or 1:10 (the lowest ones). The initial particle number concentration is 1000 cm^{-3} . Solid curves refers to the Aitken mode and dashdot curves to the accumulation mode sulphate mass fractions. Dashed curves to the Aitken mode and dotted curves to the accumulation mode organic mass fractions.

sulphate and organic particles present originally in the Aitken mode grew into the accumulation mode after 7–8 hours, and if the vapour concentration was 10^9 molecules cm^{-3} the respective growth took only 1–2 hours. At that stage, these particles can no longer be called Aitken mode particles. The original accumulation mode particles have also grown but are still in the accumulation mode size range ($< 2.5 \mu\text{m}$). As a summary, at the end of the simulation the particle population consisted of two accumulation modes with

the particles possessing different compositions as shown in Fig. 3.

The mass of particles having a diameter smaller than 100 nm ($\text{PM}_{0.1}$), smaller than $1 \mu\text{m}$ ($\text{PM}_{1.0}$) and smaller than $2.5 \mu\text{m}$ ($\text{PM}_{2.5}$) is strongly dependent on the condensing vapour concentrations and also the water content (Fig. 7). The jump, for example, in the $\text{PM}_{0.1}$ -curves in this figure shows the time when the particles have grown larger than 100 nm in diameter and when they should be called accumulation mode particles (cf. Fig. 6).

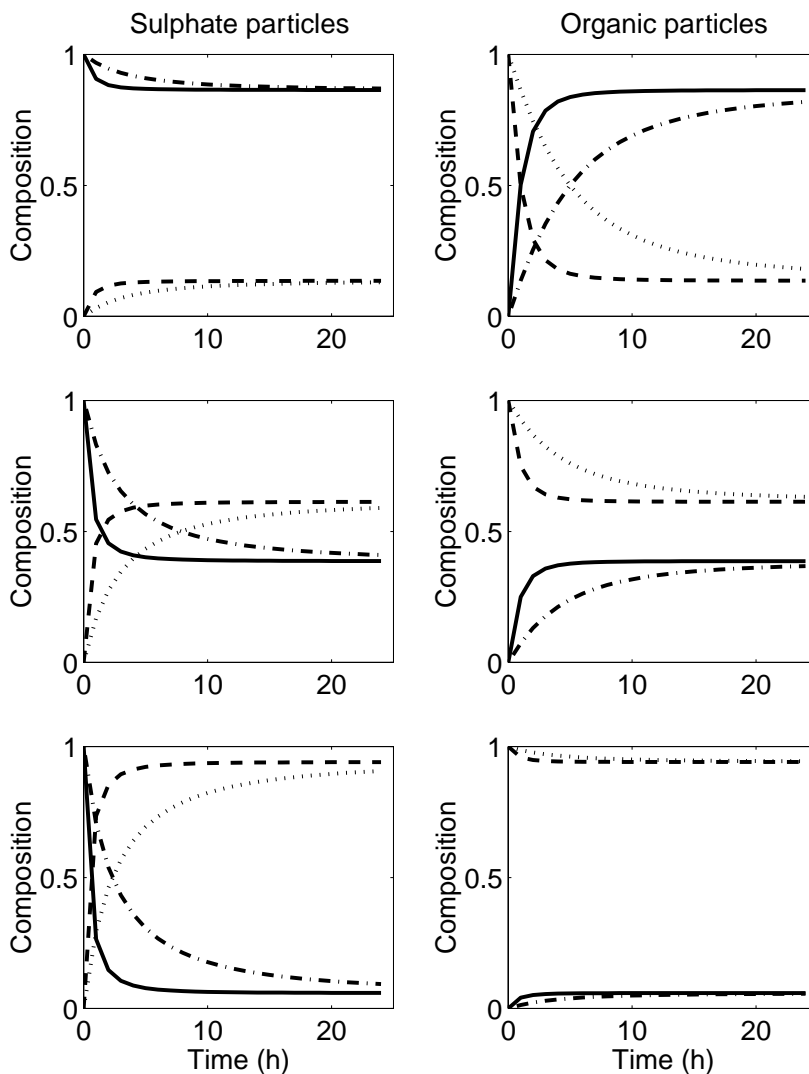


Fig. 4. As Fig. 3 but the total condensable vapour concentration is equal to 10^8 molecules cm^{-3} .

Comparison between the models MULTIMONO, MONO32, and AEROFOR2

The model MONO32 is a simplified version of the model MULTIMONO and is suitable for the use in three-dimensional Eulerian models, for example the EMEP Eulerian model MADE50 (Multi-level Acid Deposition model for Europe; e.g. Berge 1997, Berge and Jakobsen 1998). In MONO32, the four size modes (the nucleation,

the Aitken, the accumulation, and the coarse mode) are chosen as in MULTIMONO, but there is no separation for particles possessing different compositions in each size mode as in Table 1. Instead, all particles for example in the Aitken mode have the same composition, and the total masses of different compounds in this mode are calculated. Seven prognostic variables per each size mode are needed to take care of the total mass of sulphuric acid, ammonium sulphate, ammonium nitrate, organic carbon, elemental carbon,

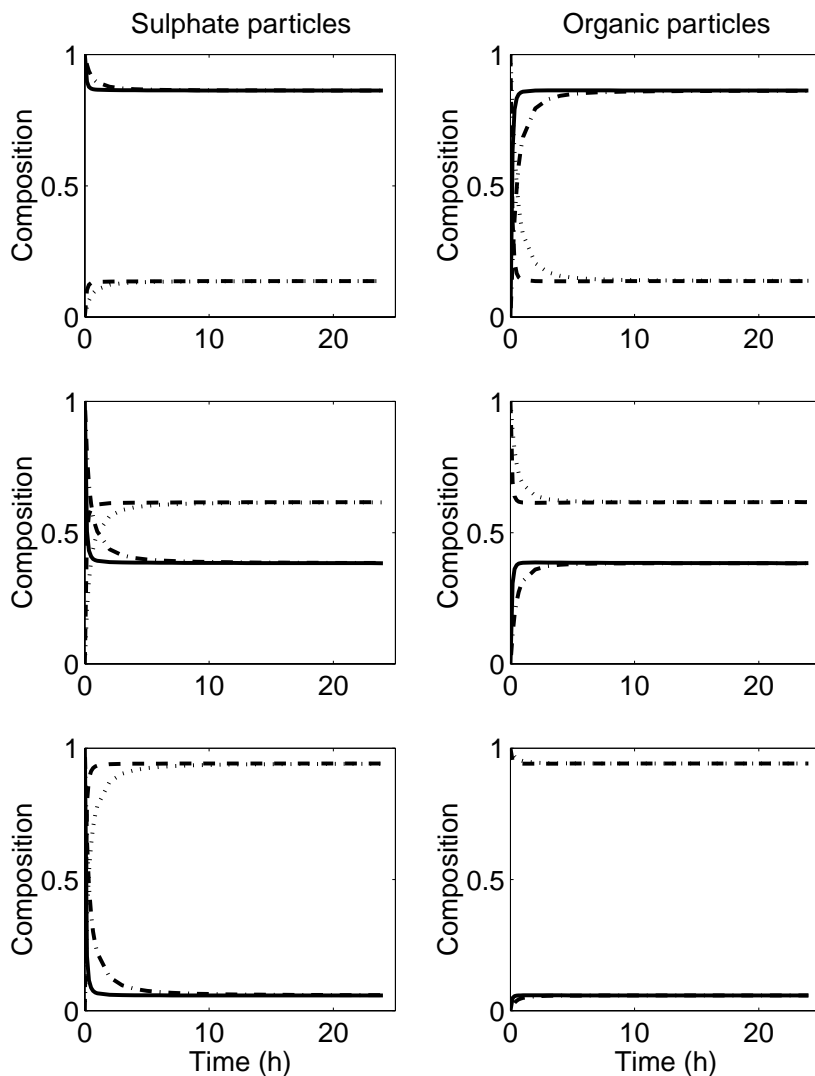


Fig. 5. As Fig. 3 but the total condensable vapour concentration is equal to 10^9 molecules cm^{-3} .

sea salt, and dust. The water content and the wet radii of the particles are calculated as in MULTIMONO. Thus the total number of differential equations for the number and the mass concentrations is only $4 + 7 \times 4 = 32$, instead of 160 in MULTIMONO.

MONO32 is useful for three-dimensional modelling because it limits the number of necessary prognostic equations and can still be used in estimating the concentrations of $\text{PM}_{2.5}$ and PM_{10} in Europe. It does not provide the possibility to investigate how rapidly internally-mixed aerosols change to externally-mixed ones, or vice versa.

The model AEROFOR2 (Pirjola and Kulmala 2000) is a sectional Lagrangian type box model

that includes atmospheric chemistry and aerosol dynamics. The particles can consist of soluble and insoluble material, and the particle population can be externally or internally mixed. The chemistry mechanism and the nucleation mechanisms are the same as in MULTIMONO and MONO32. Coagulation, dry deposition, and multicomponent condensation of sulphuric acid and organic vapour are taken into account. The model calculates the number size distribution and composition distribution of particles as a function of time.

To compare the models, a lot of simulations were carried out and the results were compared with each other. Four cases having sufficiently different conditions were chosen for this work.

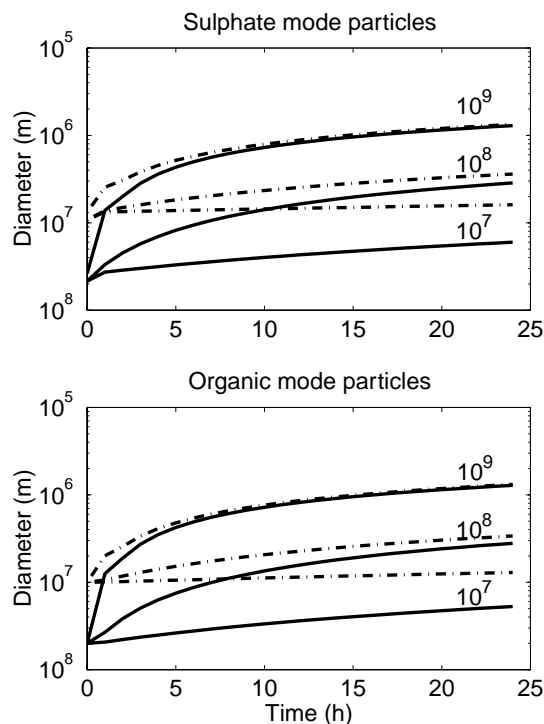


Fig. 6. Time evolution of the wet diameter of originally pure Aitken and accumulation mode sulphate and organic particles. The condensable vapour concentration is equal to 10^7 , 10^8 , or 10^9 molecules cm^{-3} . The initial particle number concentration is 1000 cm^{-3} , and the ratio of sulphate to organic particles is 10:1. Solid curves refer to the Aitken mode and dash-dot curves to the accumulation mode.

The temperature and the relative humidity had constant values of 293 K and 50%, respectively. At the beginning of each 24-hour simulation, half of the particles were pure sulphate particles and the other half were pure organic particles. The particle concentration ratio between the Aitken and the accumulation mode was 4:1 for both sulphate and organic particles, and the initial dry diameters of these two modes equal to 20 nm and 100 nm, respectively. The total particle number concentration was 10^3 and 10^5 particles cm^{-3} for slow and for faster coagulation, respectively. In addition, the geometric standard deviation of the mode needed in AEROFOR2 was chosen to be equal to 1.01 for both the modes.

In the first two cases, the concentration of condensable vapours was zero, so only coagulation and, to a minor extent, dry deposition affected

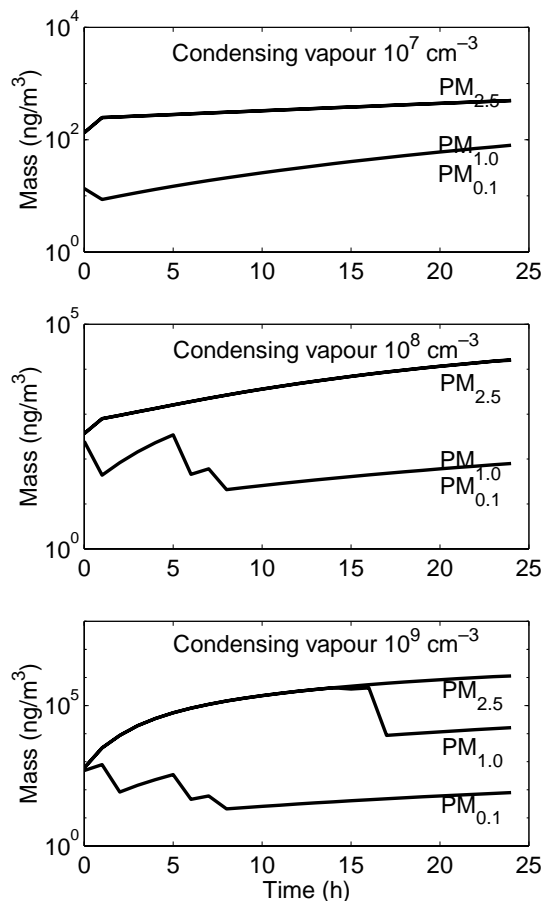


Fig. 7. Time evolution of the masses $\text{PM}_{0.1}$, $\text{PM}_{1.0}$, and $\text{PM}_{2.5}$. The condensable vapour concentration is equal to 10^7 , 10^8 , or 10^9 molecules cm^{-3} , and the ratio between the sulphuric acid and the organic vapour concentration is 10:1. The initial particle number concentration is 1000 cm^{-3} , and the ratio of sulphate to organic particles is 10:1.

the particle number concentration (Fig. 8a and b). In the second two cases, a condensable vapour concentration of 10^8 molecules cm^{-3} (half of that was sulphuric acid and the other half organic vapour) was assumed. When condensable vapours are added, particles grow faster and coagulation becomes slower (Fig. 8c and d). The results of MULTIMONO and MONO32 are almost similar and in good agreement with AEROFOR2. The difference in N_{tot} between AEROFOR2 and MULTIMONO is in maximum $\sim 5\%$.

The time evolution of the sulphate mass fraction of the whole aerosol population was also investigated. When condensable vapours were

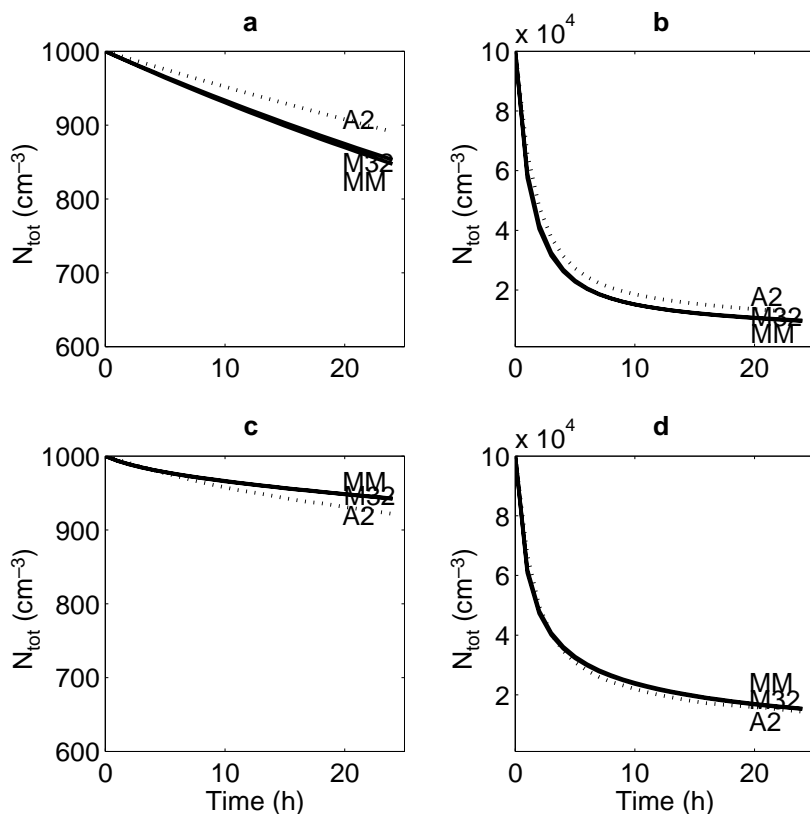


Fig. 8. Model comparisons of the time evolution of the total particle concentration. MM = MULTIMONO, M32 = MONO32 and A2 = AEROFOR2. — a: Initial $N_{\text{tot}} = 10^3$ cm⁻³ and condensable vapours = 0. — b: Initial $N_{\text{tot}} = 10^5$ cm⁻³ and condensable vapours = 0. — c: Initial $N_{\text{tot}} = 10^3$ cm⁻³, and both the sulphuric acid and organic vapour concentrations are 5×10^7 molecules cm⁻³. — d: Initial $N_{\text{tot}} = 10^5$ cm⁻³, and both the sulphuric acid and organic vapour concentrations are 5×10^7 molecules cm⁻³.

present, the sulphate fraction predicted by AEROFOR2 decreased slightly more rapidly than the fractions predicted by the monodisperse models, so that the final values were 0.46 and 0.47, respectively. If condensable vapours were not present, coagulation did not change the particle composition in spite of affecting the total particle number concentration. As a conclusion, the sulphate fractions remained practically the same in each of the models.

Conclusion

In the present paper we have developed two simple and computationally effective models (MULTIMONO and MONO32) that simulate aerosol dynamics and gas phase chemistry, especially the formation and subsequent growth of aerosol particles, as well as the evolution of the particle number and mass concentrations and the particle composition. The models can be used as sub-models in one-dimensional boundary layer models and

in three-dimensional Eulerian models.

The developed models have been compared with a more detailed sectional model AEROFOR2 (Pirjola and Kulmala 2000), and the comparisons showed that the developed models are physically sound.

The performed model runs showed that the composition of aerosol particles depends mainly on emissions and condensation. Coagulation processes seem to be of minor importance. The particle mixing state can be effectively studied using MULTIMONO or MONO32, since the degree of internal mixing depends on the condensation rate and the condensation time. On the other hand, by studying the degree of internal mixing one can examine the condensation rates.

References

- Ackermann I.J., Hass H., Memmesheimer M., Ebel A., Binkowski F.S. & Shankar U. 1998. Modal aerosol dynamics model for Europe: Development and first applications. *Atmos. Environ.* 32: 2981–2999.

- Berge E. 1997. Transboundary air pollution in Europe. MSC-W Status Report 1997, Part 1 and 2. EMEP/MSW Report 1/97. The Norwegian Meteorological Institute, Oslo, Norway.
- Berge E. & Jakobsen H.A. 1998. A regional scale multi-layer model for the calculation of long term transport and deposition of air pollution in Europe. *Tellus* 50B: 205–223.
- Chan K.C., Flagan R.C. & Seinfeld J.H. 1992. Water activities of $\text{NH}_4\text{NO}_3/(\text{NH}_4)_2\text{SO}_4$ solutions. *Atmos. Environ.* 26A: 1661–1673.
- Charlson R.J., Schwartz S.E., Hales J.M., Cess R.D., Coakley J.A., Hansen J.E. & Hofmann D.J. 1992. Climate forcing by anthropogenic aerosols. *Science* 255: 423–430.
- Chuang C.C., Penner J.E., Taylor K.E., Grossman A.S. & Walton J.J. 1997. An assessment of the radiative effects of anthropogenic sulfate. *J. Geophys. Res.* 102: 3761–3778.
- Clarke A.D. 1992. Atmospheric nuclei in the remote free troposphere. *J. Atmos. Chem.* 14: 479–488.
- Clarke A.D., Kapustin V.N., Eisele F.L., Weber R.J. & McMurry P.H. 1999. Particle production near marine clouds: Sulfuric acid and predictions from classical binary nucleation. *Geophys. Res. Lett.* 26: 2425–2428.
- Covert D.S., Kapustin V.N., Quinn P.K. & Bates T.S. 1992. New particle formation in the marine boundary layer. *J. Geophys. Res.* 97: 20581–20587.
- Dick W.D., Saxena P. & McMurry P.H. 2000. Estimation of water uptake by organic compounds in submicron aerosols measured during the Southeastern aerosol and visibility study. *J. Geophys. Res.* 101: 1471–1479.
- Dockery D.W. & Pope C.A. 1994. Acute respiratory effects of particulate air pollution. *Annu. Rev. Public Health* 15: 107–132.
- Finlayson-Pitts B.J. & Pitts J.N.Jr. 2000. *Chemistry of the upper and lower atmosphere*. Academic Press, New York, 969 pp.
- FORTTRAN-routine D02EAF 1990. *The NAG workstation library handbook 1*. The Numerical Algorithms Group Ltd., Oxford.
- Fuchs N.A. 1964. *The mechanics of aerosols*, Pergamon Press, London.
- Fuchs N.A. & Sutugin A.G. 1970. *Highly dispersed aerosol*. Ann Arbor Science Publi., Ann Arbor Michigan, 105 pp.
- Griffin R.J., Crocker D.R.III, Flagan R.C. & Seinfeld J.H. 1999. Organic aerosol formation from the oxidation of biogenic hydrocarbons. *J. Geophys. Res.* 104: 3555–3567.
- Haywood J. M. & Ramaswamy V. 1998. Global sensitivity studies of the direct radiative forcing due to anthropogenic sulfate and black carbon aerosols. *J. Geophys. Res.* 103: 6043–6058.
- Harrington D.Y. & Kreidenweis S.M. 1998a. Simulations of sulfate aerosol dynamics — 1. Model description. *Atmos. Environ.* 32: 1691–1700.
- Harrington D.Y. & Kreidenweis S.M. 1998b. Simulations of sulfate aerosol dynamics. Part II. Model inter-comparison. *Atmos. Environ.* 32: 1701–1709.
- Hegg D.A., Radke L.F. & Hobbs P.V. 1991. Measurements of Aitken nuclei and cloud condensation nuclei in the marine atmosphere and their relation to the DMS-cloud-climate hypothesis. *J. Geophys. Res.*, 96: 18727–18733.
- Hoffmann T., Bandur R., Marggraf U. & Linscheid M. 1998. Molecular composition of organic aerosols formed in the α -pinene/ O_3 reaction: Implications for new particle formation processes. *J. Geophys. Res.* 103: 25569–25578.
- Hoppel W.A., Frick G.M., Fitzgerald J.W. & Larson R.E. 1994. Marine boundary layer measurements of new particle formation and the effects nonprecipitating clouds have on aerosol size distribution. *J. Geophys. Res.* 99: 14443–14459.
- Jang M. & Kamens R.M. 1999. Newly characterized products and composition of secondary aerosols from the reaction of α -pinene with ozone. *Atmos. Environ.* 33: 459–474.
- Jaecker-Voirol A., Mirabel P. & Reiss H. 1987. Hydrates in supersaturated binary sulphuric acid-water vapor: A reexamination. *J. Chem. Phys.* 87: 4849–4852.
- Kaufman Y.J. & Fraser R.S. 1997. The effect of smoke particles on clouds and climate forcing. *Science* 277: 1636–1639.
- Kerminen V.-M. & Wexler A.S. 1996. The occurrence of sulfuric acid-water nucleation in plumes: Urban environment. *Tellus* 48B: 65–82.
- Kerminen V.-M. 1999. Roles of SO_2 and secondary organics in the growth of nanometer particles in the lower atmosphere. *J. Aerosol Sci.* 30: 1069–1078.
- Kerminen V.-M., Pirjola L., Boy M., Eskola A., Teinilä K., Laakso L., Asmi A., Hienola J., Lauri A., Vainio V., Lehtinen M. & Kulmala M. 2000a. Interaction between SO_2 and submicron atmospheric particles. *Atmos. Res.* 54: 49–57.
- Kerminen V.-M., Virkkula A., Hillamo R., Wexler A.S. & Kulmala M. 2000b. Secondary organics and atmospheric cloud condensation nuclei production. *J. Geophys. Res.* 105: 9255–9264.
- Korhonen P., Kulmala M., Laaksonen A., Viisanen Y., McGraw R. & Seinfeld J.H. 1999. Ternary nucleation of H_2SO_4 , NH_3 , and H_2O in the atmosphere. *J. Geophys. Res.* 104: 26349–26353.
- Kulmala M., Kerminen V.-M. & Laaksonen A. 1995. Simulations on the effect of sulphuric acid formation on atmospheric aerosol concentrations. *Atmos. Environ.* 29: 377–382.
- Kulmala M., Toivonen A., Mäkelä J.M. & Laaksonen A. 1998a. Analysis of the growth of nucleation mode particles in Boreal Forest. *Tellus* 50B: 449–462.
- Kulmala M., Laaksonen A. & Pirjola L. 1998b. Parameterizations for sulphuric acid/water nucleation rates. *J. Geophys. Res.* 103: 8301–8308.
- Kulmala M., Pirjola L. & Mäkelä J.M. 2000. Stable sulphate clusters as a source of new atmospheric particles. *Nature* 404: 86–89.

- Mäkelä J.M., Aalto P., Jokinen V., Pohja T., Nissinen A., Palmroth S., Markkanen T., Seitsonen K., Lihavainen H. & Kulmala M. 1997. Observations of ultrafine aerosol particle formation and growth in boreal forest. *Geophys. Res. Lett.* 24: 1219–1222.
- O'Dowd C.D., Geever M., Hill M.K., Smith M.H. & Jennings S.G. 1998. New particle formation: Nucleation rates and spatial scales in the clean marine coastal environment. *Geophys. Res. Letts.* 25: 1661–1664.
- O'Dowd C.D., McFiggens G., Pirjola L., Creasey D.J., Hoell C., Smith M.H., Allen B., Plane J.M.C., Heard D.E., Lee J.D., Pilling M.J. & Kulmala M. 1999. On the photochemical production of new particles in the coastal boundary layer. *Geophys. Res. Letts.* 26: 1707–1710.
- Pirjola L. & Kulmala M. 1998. Modelling the formation of H₂SO₄-H₂O particles in rural, urban and marine conditions. *Atmos. Res.* 46: 321–347.
- Pirjola L., Laaksonen A., Aalto P. & Kulmala M. 1998. Sulfate aerosol formation in the Arctic boundary layer. *J. Geophys. Res.* 103: 8309–8322.
- Pirjola L., Kulmala M., Wilck M., Bischoff A., Stratmann F. & Otto E. 1999. Effects of aerosol dynamics on the formation of sulphuric acid aerosols and cloud condensation nuclei. *J. Aerosol Sci.* 30: 1079–1094.
- Pirjola L. 1999. Effects of the increased UV radiation and biogenic VOC emissions on ultrafine aerosol formation. *J. Aerosol. Sci.* 30: 355–367.
- Pirjola L. & Kulmala M. 2000. Development of particle size and composition distribution with aerosol dynamics model AEROFOR2. *Report Series in Aerosol Science* 47: 174–186.
- Pitchford M.L. & Mc Murry P.H. 1994. Relationship between measured water vapor growth and chemistry of atmospheric aerosol for Grand Canyon, Arizona, in winter 1990. *Atmos. Environ.* 28: 827–839.
- Raes F., van Dingenen R., Cuevas E., van Velthoven P.F.J. & Prospero J.M. 1997. Observations of aerosols in the free troposphere and marine boundary layer of the subtropical Northeast Atlantic: Discussion of processes determining their size distribution. *J. Geophys. Res.* 102: 21315–21328.
- Reid R.C., Prausnitz J.M. & Poling B.E. 1987. *The Properties of Gases and Liquids*, 4th edition. McGraw-Hill, New York, 741 pp.
- Saxena P. & Hildemann L.M. 1996. Water-soluble organics in atmospheric particles: A critical review of the literature and application of thermodynamics to identify candidate compounds. *J. Atmos. Chem.* 24: 57–109.
- Saxena P. & Hildemann L.M. 1997. Water absorption by organics: Survey of laboratory evidence and evaluation of UNIFAC for estimating water activity. *Environ. Sci. Technol.* 31: 3318–3324.
- Schack C.J.Jr., Pratsinis S.E. & Friedlander S.K. 1985. A general correlation for deposition of suspended particles from turbulent gases to completely rough surfaces. *Atmos. Environ.* 19: 953–960.
- Schröder F. & Ström J. 1997. Aircraft measurements of submicrometer aerosol particles (> 7 nm) in the mid-latitude free troposphere and tropopause region. *Atmos. Res.* 44: 333–356.
- Seinfeld J.H. & Pandis J.S. 1998. *Atmospheric chemistry and physics. From air pollution to climate change*. John Wiley & Sons, Inc. New York, 1326 pp.
- Simpson D. 1992. Long-period modelling of photochemical oxidants in Europe. Model calculation for July 1985. *Atmos. Environ.* 26A: 1609–1634.
- Sokolik I.N. & Toon O.B. 1996. Direct radiative forcing by anthropogenic airborne mineral aerosols. *Nature* 381: 681–683.
- Tang I.N. & Munkelwitz H.R. 1994. Water activities, densities, and refractive indices of aqueous sulfates and sodium nitrate droplets of atmospheric importance. *J. Geophys. Res.* 99: 18801–18808.
- Weber R.J., McMurry P.H., Mauldin R.L., Tanner D., Eisele F.L., Brechtel F., Kreidenweis S., Kok G., Schillawski R. & Baumgardner D. 1998. A study of new particle formation and growth involving biogenic trace gas species measured during ACE-1. *J. Geophys. Res.* 103: 16385–16396.
- Weber R.J., McMurry P.H., Mauldin R.L., Tanner D., Eisele F.L., Clarke A.D. & Kapustin V. 1999. New particle formation in the remote troposphere: A comparison of observations at various sites. *Geophys. Res. Lett.* 26: 307–310.
- Wiedensohler A., Covert D.S., Swietlicki E., Aalto P., Heintzenberg J. & Leck C. 1996. Occurrence of an ultrafine particle mode less than 20 nm in diameter in the marine boundary layer during Arctic summer and autumn. *Tellus* 48B: 213–222.
- Viisanen Y., Kulmala M. & Laaksonen A. 1997. Experiments on gas-liquid nucleation of sulfuric acid and water. *J. Chem. Phys.* 107: 920–926.
- Wilemski G. 1984. Composition of the critical nucleus in multicomponent vapor nucleation. *J. Chem. Phys.* 80: 1370–1372.
- Winter B. & Chylek P. 1997. Contribution of sea salt aerosol to the planetary clear-sky albedo. *Tellus* 49B: 72–79.
- Virkkula A., Van Dingenen R., Raes F. & Hjorth J. 1998. Hygroscopic properties of aerosol formed by oxidation of limonene, α -pinene and β -pinene. *J. Geophys. Res.* 104: 3569–3579.